sciendo

Theoretical investigation of aniline derivatives: Correlation of theoretical reaction Gibbs free energies with experimental oxidation potentials

Andrea Kováčová, Martin Michalík

Institute of Physical Chemistry and Chemical Physics, Slovak University of Technology in Bratislava, Radlinského 9, SK–812 37 Bratislava, Slovakia
andrea.kovacova@stuba.sk

Abstract: Anilines and their derivatives are used in industrial production of dyes, pharmaceuticals, plastics, and synthetic antioxidants. Abstraction of electron and formation of a cation radical represent a significant step in the reactivity of this group of substances. The aim of this study was to theoretically investigate the effect of a substituent on the oxidative electrochemical potential of 64 species of aniline derivatives. Quantum-chemical calculations were performed using the composite G4 method. The obtained linear dependences for reaction Gibbs free energies were correlated with the Hammett constants and available experimental values.

Keywords: anilines, electrochemical potential, reaction Gibbs energies, Gn approach, thermodynamics, implicit solvent model

Introduction

In organic materials, a number of chemical processes are initiated by homolytic cleavage of chemical bonds. Reactivity and stability widely vary for such generated radicals which is the subject of many studies. In case of polymers, formation of radicals can lead either to the formation of new materials with interesting properties, i.e. cross-linked materials (Skákalová, Lukeš and Breza, 1997), or to simple degradation. Antioxidants which can trap these radicals are mostly phenol- (Kleinová et al., 2024), or aniline-based (Kováčová et al., 2023; Lukeš and Hartmann, 2021) compounds. Derivatives of the latter have a wide spectrum of applications in various industries, e.g., polymers, dyes, rubber, medicine, pharmacology, and electronics (Anjalin, Kanagathara and Baby Suganthi, 2020; Lukeš et al., 2011; Rappoport, 2007). *Para*-aniline derivatives also include hydroquinones (Rani and Shanker, 2017). Lately, Pavitt et. al published electrochemical potentials of aniline derivatives measured in water by the SCV method (Pavitt, Bylaska and Tratnyek, 2017). Their study inspired us to providing theoretical background while testing the current state-of-art calculation approach, G4.

The composite G4 method is often used as a more precise method for reference theoretical calculations, e.g. bond dissociation enthalpy (Biela et al., 2023). Needless to say, this method is much more computationally expensive as it uses a complex multi-step procedure. One of the steps involves single point calculation at the MP4 level of theory, for which 128 GB of RAM is necessary even for medium sized molecules. Still, a more conventional QSPR approach in the first step is adequate in many cases to obtain approximate classification of derivatives.

Despite being almost a century old, the Hammett constant still allows for reasonable quantification of electron-donating (negative values) or electron-withdrawing (positive values) properties of substituents. There are substituents with different effect in meta and in para position, it is also possible to use Hammett type constants (for example Brown-Okamoto (Hansch, Leo and Taft, 1991)) plus (σ^+) or minus (σ^-) for substituents in the para position. Once linear dependences are found and enumerated for a given dataset of derivatives with known properties, prediction for other compounds is possible using QSPR, e.g. BDE (Vagánek et al., 2013).

Considering the above points, the main aims of this paper are: (1) to find optimal geometries of studied molecules using steps within the G4 method; (2) to calculate reaction Gibbs free energies related to the reaction in Eq. 1; (3) to evaluate electrochemical potentials and to compare obtained values with available experimental data, and (4) to assess the substitution effect using the QSPR approach. This work is a continuation of a similar study carried out on phenolic derivatives (Kováčová, 2024).

Calculation details

Quantum-chemical calculations

Quantum-chemical calculations were performed by composite Gaussian-4 level (G4) of theory (Curtiss, Redfern and Raghavachari, 2007) as implemented in the Gaussian 09 program package (Frisch et al., 2009). For comparison, computa-

Acta Chimica Slovaca, Vol. 17, No. 1, 2024, pp. 74—82, DOI: 10.2478/acs-2024-0010

tional analyses were performed using the density functional theory at the B97D3/def2-TZVPP level (Grimme, Ehrlich and Goerigk, 2011; Weigend and Ahlrichs, 2005). The solvent effect contribution of water was simulated using SMD implicit solvent model (solvation model based on the quantum mechanical charge density of a solute molecule interacting with a continuum) (Marenich, Cramer and Truhlar, 2009). This model is based on the generalised Born equation, which is represented by an approximation of the Poisson equation suitable for arbitrary cavity shapes. Gibbs free energies were evaluated for the temperature of 298.15 K and the pressure of 101.325 kPa. Vibrational analysis included in the G4 calculation process showed no imaginary frequencies, which confirms geometry corresponding to the lowest energy minimum. Optimal geometries were visualised for the *ortho*- and *poly*-substituted aniline derivatives using the open-source Jmol viewer (Fig. 2) (Jmol development team, 2016). Pre-optimisation of some molecules was performed using the XTB program package (Bannwarth et al., 2021; Bannwarth, Ehlert and Grimme, 2019; Pracht, Bohle and Grimme, 2020). Structural schemes with notation of studied species are shown in Fig. 1.

Results and Discussion

To investigate the thermodynamics of one-electron transfer reaction according to Eq. 1

$$X—Ar—NH_2 \rightarrow (X—Ar—NH_2)^{\bullet+} + e^- \quad (1)$$

where X represents the substituents used, it was necessary to calculate the geometry of neutral molecule and the corresponding cation radical. Optimal geometries for selected *ortho*- and *poly*-substituted anilines in neutral states are depicted in Fig. 2. Reaction Gibbs free energies expressing electron abstraction ($\Delta_r G$) follow Eq. 2

$$\Delta_r G = G((X—Ar—NH_2)^{\bullet+}) - G(X—Ar—NH_2) + G(e^-) = \\ = \Delta G + G(e^-) \quad (2)$$

where $G((X—Ar—NH_2)^{\bullet+})$ and $G(X—Ar—NH_2)$ denote the Gibbs free energies of the cation radical and neutral compound, respectively, and $G(e^-)$ is the Gibbs free energy of the solvated electron. Calculated $\Delta_r G$ values for all mono-substituted anilines can be found in Tab. 1. The value of $G(e^-)$ in Eq. 2 is constant (–149 kJ · mol^{-1}) for all reactions under study. This value was calculated by adding $G(e^-)$ for vacuum (–4 kJ · mol^{-1}, (Fifen, 2013)) with a solvation correction (water) –145 kJ · mol^{-1} (Ishikawa and Nakai, 2016).

According to the thermodynamic theory and after correction to standard hydrogen electrode (SHE) (Ho et al., 2016), the absolute electrochemical potential can be calculated from the reaction Gibbs energies using Eq. 3

$$E^{cal} = -(\Delta_r G / nF) - E^{SHE} \quad (3)$$

where E^{cal} denotes electrochemical potential, $\Delta_r G$ is the reaction Gibbs free energy, n represents the number of exchange electrons in the reaction, F is the Faraday constant (96 485 C · mol^{-1}), and E^{SHE} is the absolute electrochemical potential of SHE (4.28 V). For twelve aniline derivatives, experimental values of electrochemical potential, E, are

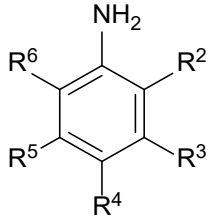

Name	Notation	Name	Notation
aniline	H	2,6-dimethylaniline	26Me
x-acetylaniline	xAc	3,4-dimethylaniline	34Me
x-bromoaniline	xBr	3,5-dimethylaniline	35Me
x-trifluoromethylaniline	xCF3	2,3-dimethoxyaniline	23OMe
x-chloroaniline	xCl	2,4-dimethoxyaniline	24OMe
x-cyanoaniline	xCN	2,5-dimethoxyaniline	25OMe
x-aminobenzaldehyde	xCOH	2,6-dimethoxyaniline	26OMe
x-aminobenzoic acid	xCOOH	3,4-dimethoxyaniline	34OMe
x-ethylaniline	xEt	3,5-dimethoxyaniline	35OMe
x-fluoroaniline	xF	2,4-dinitroaniline	24NO_2
x-methylaniline	xMe	2,4,6-trimethylaniline	246Me
x-aminoaniline	xNH2	2,4,6-trichloroaniline	246Cl
x-nitroaniline	xNO2	2,6-dinitro-4-methylaniline	4Me-26NO_2
x-nitrosoaniline	xNO	2-methoxy-4-ethylaniline	2OMe-4Et
x-methoxyaniline	xOMe	2-Hydroxy-4-methoxybenzaldehyde	2OMe-4COH
2,3-dimethylaniline	23Me	2-methyl-5-nitroaniline	2Me-5NO_2
2,4-dimethylaniline	24Me	2-methoxynitroaniline	2OMe-NO_2
2,5-dimethylaniline	25Me	4-methyl-3-nitroaniline	4Me-3NO_2

Fig. 1. Schematic structures and notations of studied molecules. X = 2 for *ortho*- derivatives, X = 3 for *meta*- derivatives and X = 4 for *para*- derivatives.

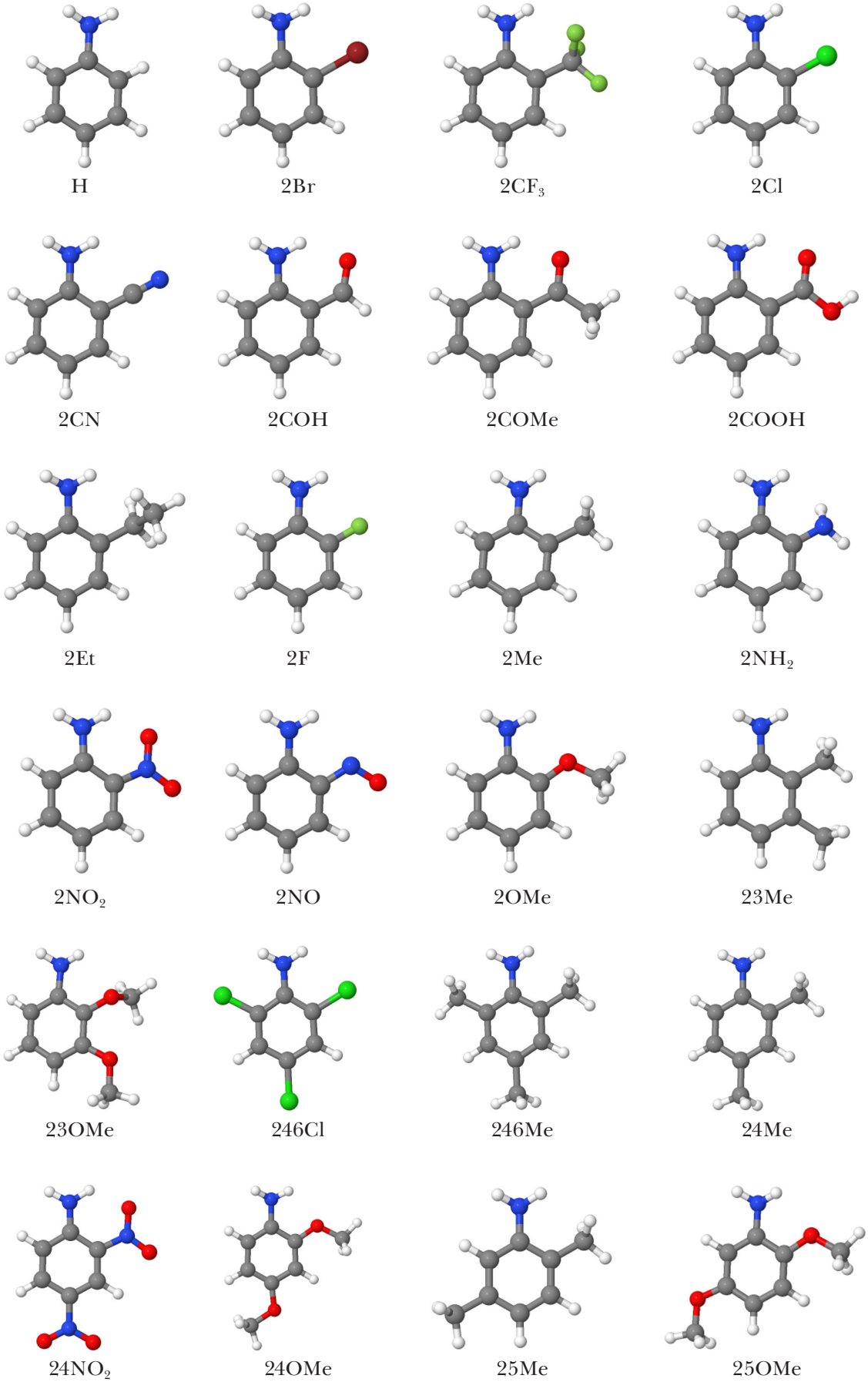

Fig. 2. G4 optimal geometries of *ortho*- and *poly*-substituted aniline derivatives.

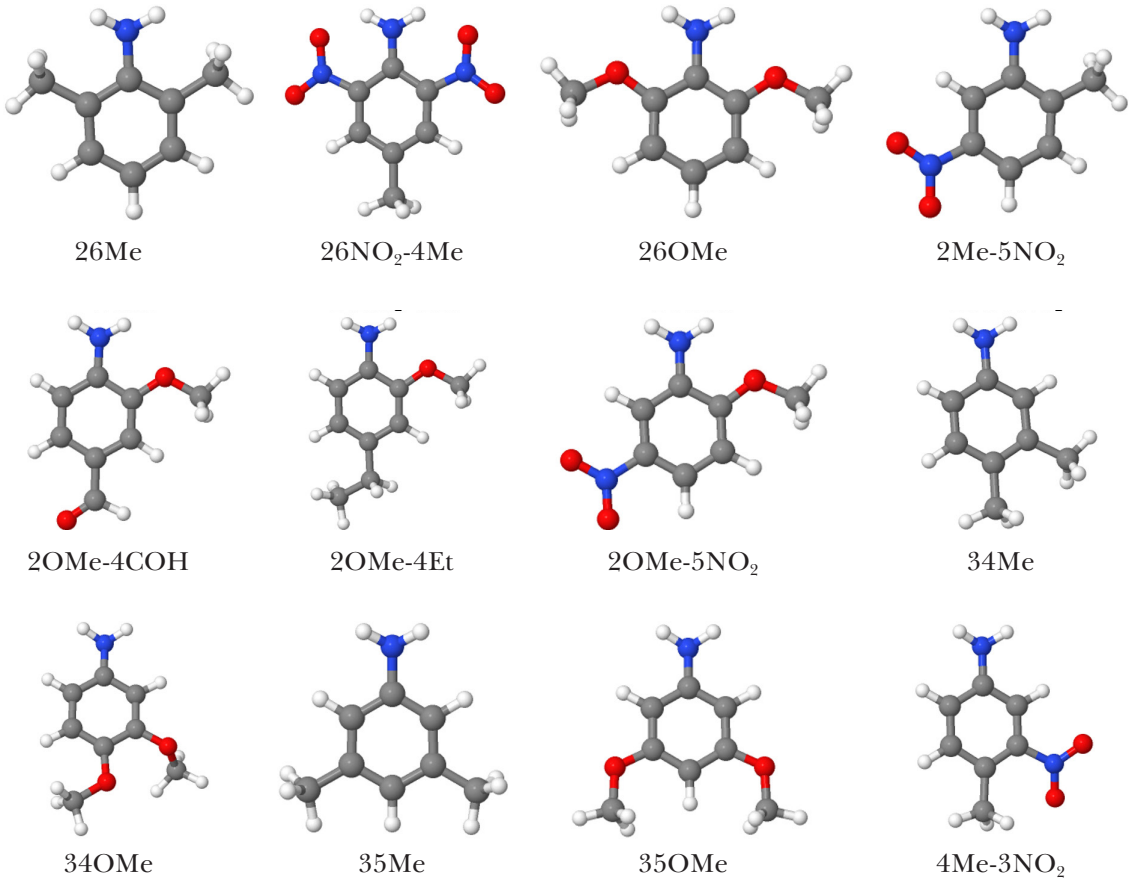

Fig. 2 continue. G4 optimal geometries of *ortho*- and *poly*-substituted aniline derivatives.

Tab. 1. Takahata-Chong Hammett type constants for *ortho* isomers (σ_o) (Takahata and Chong, 2005), and Hammett constants for *meta* (σ_m) and *para* (σ_{p+}) isomers (Hansch, Leo and Taft, 1991). Calculated G4(water) reaction Gibbs free energies for electron abstraction, experimental electrochemical potential E^{exp} vs. SHE (Pavitt, Bylaska and Tratnyek, 2017), and bond length (d) for C—N in monosubstituted anilines.

Substituent	Hammett constants			$\Delta_r G$/kJ·mol^{-1}			E^{exp}/V			d/Å		
	σ_O	σ_m	σ_{p+}	*ortho*	*meta*	*para*	*ortho*	*meta*	*para*	*ortho*	*meta*	*para*
H	0.00	0.00	0.00	369	369	369	1.07	1.07	1.07	1.394	1.394	1.394
Br		0.39	0.15	395	387	376				1.385	1.387	1.389
CF3		0.43	0.61	395	385	391				1.385	1.388	1.381
Cl	0.20	0.37	0.11	389	385	373	1.204	1.167	1.058	1.385	1.387	1.390
CN	0.71	0.56	0.66	406	397	398				1.372	1.385	1.369
COH		0.35	0.73	393	387	392				1.354	1.388	1.363
COMe		0.38		382	380	390				1.358	1.391	1.369
COOH		0.37	0.42	389	385	392		1.074	1.122	1.363	1.389	1.370
Et	–0.31	–0.07	–0.30	357	368	357				1.398	1.395	1.397
F	0.24	0.34	–0.07	383	382	367				1.392	1.388	1.398
Me	–0.17	–0.07	–0.31	363	363	352	1.017	1.029	0.927	1.396	1.395	1.398
NH_2	–0.41	–0.16	–1.30	325	342	296				1.405	1.396	1.408
NO_2	0.80	0.71	0.79	415	401	409	1.372	1.269	1.35	1.345	1.383	1.350
NO		0.62		386	401	389				1.343	1.385	1.344
OMe	–0.39	0.12	–0.78	349	369	325	0.894	1.023	0.766	1.397	1.393	1.403

available, ranging from 0.63 V for $4NH_2$ derivate (electron-donor) to 1.26 V for 4COH and 2CN derivatives (electron-acceptor), see Tab. 1.

In Fig. 3, the dependence between Takahata-Chong or Hammett constants and E^{exp} experimental values for *ortho*-, *meta*-, and *para*- derivatives, combined is shown. Coefficient of determination (R^2) of 0.915 was found from linear regression. Line parameters *a*, *b* with errors are summarised in Tab. 2.

The substituent constants however work best only for mono-substituted derivatives. Another descriptor, which does not have this limitation might be the C—N bond length, where N is amino nitrogen of neutral derivatives. While the changes are quite subtle, good correlation was found with E^{exp} and R^2 of 0.927 for 14 points (Fig. 5). The shorter the bond, the more is the lone pair of nitrogen involved in benzene ring conjugation. The trend does not follow substituents with the strongest effect on the ring, i.e., $2NO_2$, $4NO_2$, and 4COOH derivatives. On the other hand, if also *poly*-substituted anilines are included in the theoretical $\Delta_r G$ values, even better correlation can be found. Depicted in Fig. 4 (a) for 18 points, the value of R^2 is 0.955. Interestingly, for 5 *ortho* derivatives, the coefficient of determination even reached 0.993, which is not the case for *meta* and *para* derivatives.

A comparison between the linear correlations based on the B97D3/def2-TZVPP level of theory data presented in Fig. 4(b) and the original data set (see Tab. 2) revealed similar line parameters. Nevertheless, the coefficients of determination are slightly lower (R^2 of 0.939). However, it should be noted, that DFT takes only ca. 10 % of the overall computational time of the G4 method.

This relationship naturally arises from Eq. 3, but the intercepts found are far from the value of SHE electrochemical potential. In fact, electrochemical potentials, E^{cal}, for all anilines under study can be directly calculated based on Eq. 3 and compared with available data. A comparison of the three methods of theoretical prediction of electrochemical potential is shown in Fig. 6. While individual values obtained from correlation methods ($E^{\Delta G}$, E^{σ}) are relatively close to each other, E^{cal} values show large discrepancies. This might be attributed to the varying experimental conditions e.g., overpotential of the electrode, which is included in the regression models $E^{\Delta G}$ and E^{σ} trained on experimental data. The shift from experimental values is largely consistent when experimental conditions remain constant. Consequently, data from diverse sources with varying conditions may not be compatible. It can be argued that values scaling is a common practice in theoretical modelling, as it facilitates better correlation with experiments often correcting shortcomings of the implicit solvation model. Thermodynamic quantities, such as pK_a (Busch et al., 2022), bond dissociation energies (Bakalbassis, Lithoxoidou and Vafiadis, 2003), and ionisation potential (Fu et al., 2005), are particularly characteristic of this phenomenon, whereby computed theoretical values are mapped onto experimental ones. Some improvement is expected if explicit solvent molecules are added, but calculations including advanced explicit solvation models are beyond the scope of this paper.

Conclusion

In this study, the effect of a substituent on the oxidative electrochemical potential of 64 species of aniline derivatives has been theoretically investigated. The results presented here were obtained

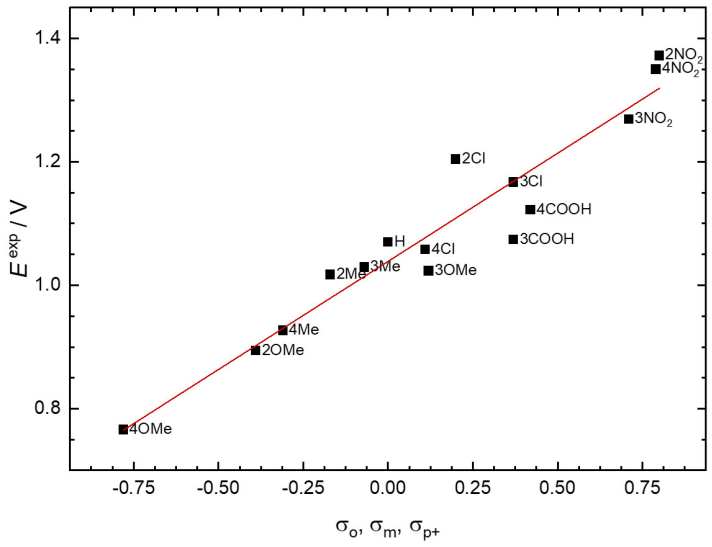

Fig. 3. Dependence of electrochemical potentials on Takahata-Chong Hammett type constants (*ortho*- derivatives) and Hammett constants (*meta*, *para*) for aniline derivatives.

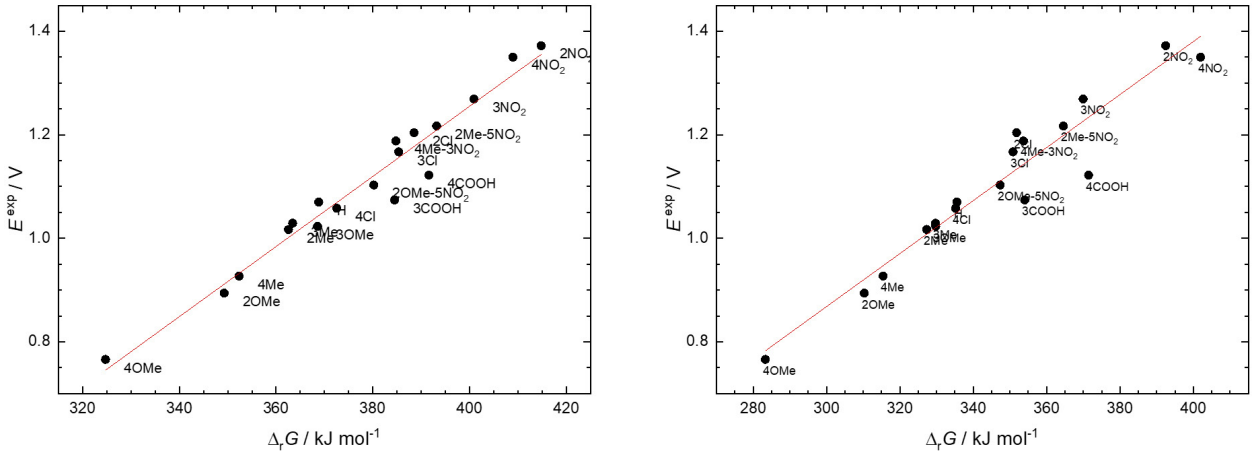

a) b)

Fig. 4. Dependence of electrochemical potentials on reaction Gibbs free energies by (a) G4 method and (b) DFT-D3 level of theory.

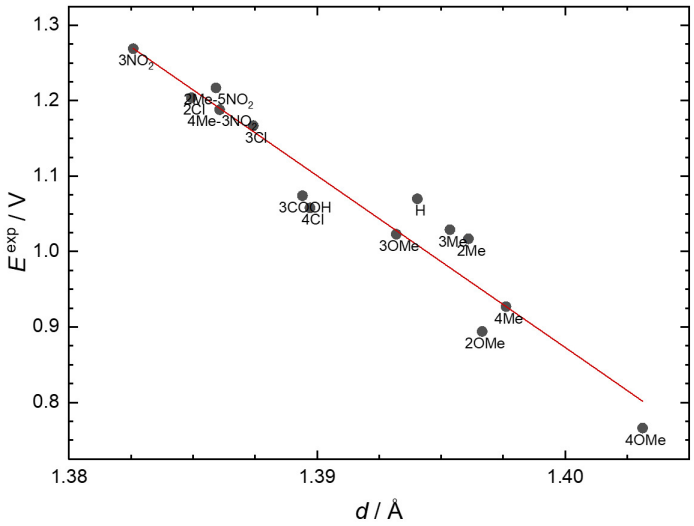

Fig. 5. Dependence of available experimental values of electrochemical potentials on C—N bond length (G4 method).

Tab. 2. a, b parameters with errors and coefficient of determination (R^2) for linear correlations described by equations E/V = a + b × ΔG/kJ·mol^{-1}, E/V = a + b × σ or E/V = a + b × d/Å, respectively, for *ortho*- (E_o), *meta*- (E_m), *para*- (E_p), and *poly*-substituted (E_{poly}) anilines. B97D3 denotes DFT data, otherwise, data from the G4 method are employed.

	a	***b* 10^{-3}**	**n**	**R^2**
$E_{o,\Delta G}$	–1.58 ±0.13	7.15 ±0.34	5	0.993
$E_{m,\Delta G}$	–1.24 ±0.50	6.2 ±1.3	6	0.846
$E_{p,\Delta G}$	–1.35 ±0.25	6.49 ±0.67	6	0.959
$E_{poly,\Delta G}$	–1.31 ±0.62	6.4 ±1.6	4	0.885
$E_{\Delta G}$	–1.45 ±0.14	6.77 ±0.37	18	0.955
$E_{\Delta G,B97D3}$	–0.71 ±0.12	5.24 ±0.33	18	0.939
E_{σ}	1.039 ±0.014	350 ±30	15	0.915
E_{d}	32.8 ±2.6	–22800 ±1800	14	0.927
$E_{d,B97D3}$	29.4 ±3.3	-20400 ±2400	14	0.859

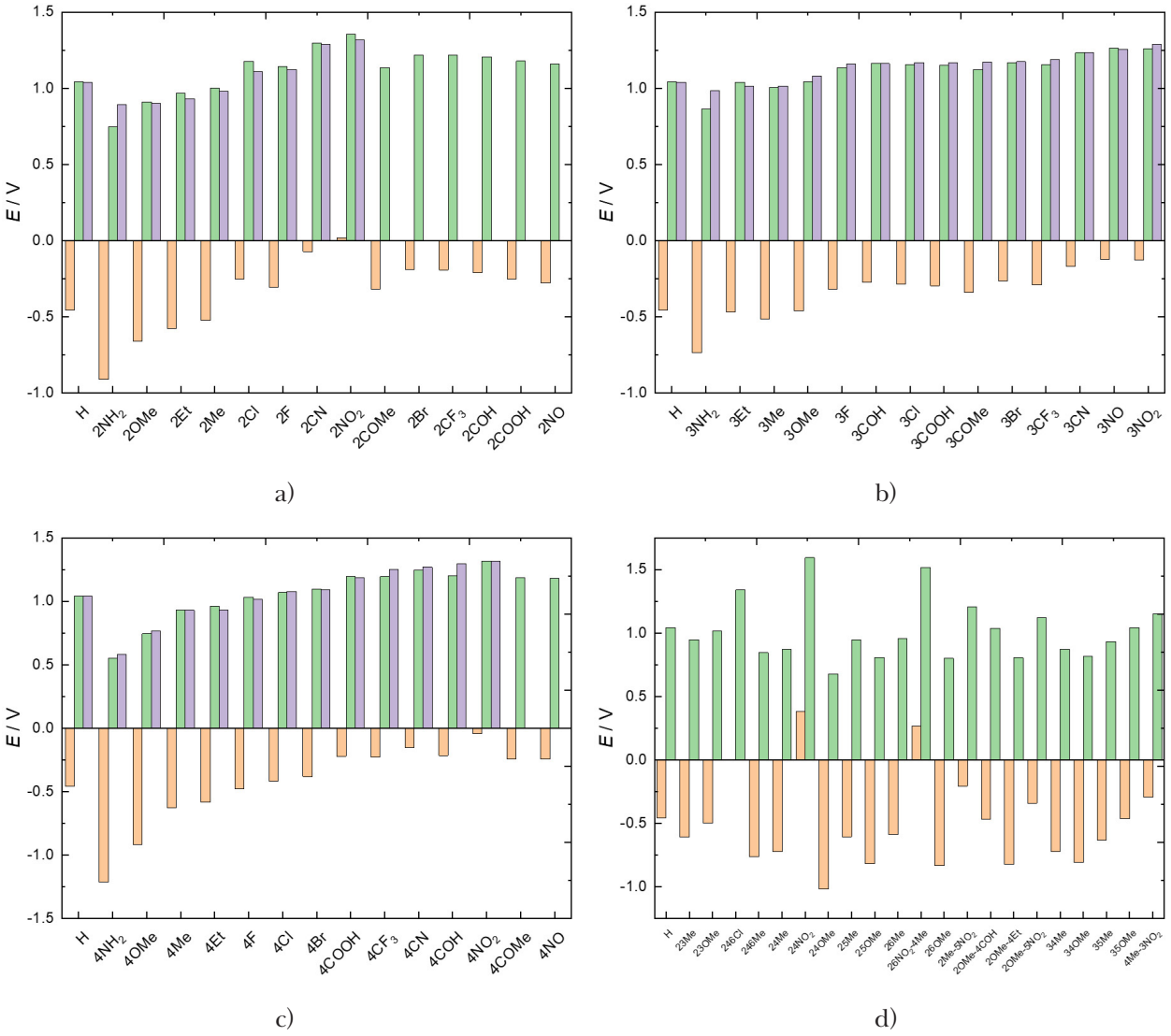

Fig. 6. Comparison of G4 calculated electrochemical potentials E^{cal} (orange), $E^{\Delta G}$ (green), E^{σ} (purple) for selected substituents. Values of E^{σ} were calculated for substituents with available Hammett constants only.

Tab. 3. Calculated G4(water) reaction Gibbs free energies ($\Delta_r G$) for electron abstraction, experimental electrochemical potential (E^{exp}) vs. SHE (Pavitt, Bylaska and Tratnyek, 2017) and bond length (d) for C—N of *poly*-substituted aniline derivatives.

Substituent	$\Delta_r G$/kJ·mol^{-1}	E^{exp}/V	d/Å	Substituent	$\Delta_r G$/kJ·mol^{-1}	d/Å
24N$_O$2	450		1.333	**23OMe**	365	1.392
2OMe-5NO$_2$	380	1.103	1.386	**24OMe**	315	1.405
4Me-26NO$_2$	439		1.331	**25OMe**	334	1.394
2Me-5NO$_2$	393	1.217	1.386	**26OMe**	333	1.400
23Me	354		1.398	**34OMe**	335	1.401
24Me	343		1.399	**35OMe**	368	1.393
25Me	355		1.397	**2OMe-4Et**	334	1.399
26Me	356		1.397	**2OMe-4CHO**	368	1.367
34Me	343		1.399	**246Me**	339	1.401
35Me	352		1.397	**246Cl**	413	1.373
4Me-3NO$_2$	385	1.188	1.386			

Tab. 4. Calculated B97D3/def2-TZVPP reaction Gibbs free energies for electron abstraction and bond length (*d*) for C—N of monosubstituted anilines.

Substituent	$\Delta_r G_{B97D3}$/kJ·mol^{-1}			*d*/Å		
	ortho	*meta*	*para*	*ortho*	*meta*	*para*
H	336	336	336	1.393	1.393	1.393
Br	359	353	338	1.383	1.387	1.389
CF3	366	356	364	1.381	1.387	1.378
Cl	352	351	335	1.384	1.387	1.390
CN	375	365	371	1.369	1.384	1.367
COH	373	359	375	1.351	1.386	1.358
COMe	359	352	364	1.355	1.390	1.365
COOH	362	354	371	1.360	1.388	1.366
Et	326	338	320	1.396	1.395	1.398
F	346	348	330	1.389	1.387	1.397
Me	327	330	315	1.395	1.395	1.398
NH_2	285	298	254	1.404	1.396	1.409
NO_2	392	370	402	1.345	1.381	1.348
NO	345	365	333	1.342	1.383	1.343
OMe	310	330	283	1.395	1.394	1.402

Tab. 5. Calculated B97D3/def2-TZVPP reaction Gibbs free energies for electron abstraction and bond length (*d*) for C—N *of poly*-substituted aniline derivatives.

Substituent	$\Delta_r G_{B97D3}$/kJ·mol^{-1}	*d*/Å	Substituent	$\Delta_r G_{B97D3}$/kJ·mol^{-1}	*d*/Å
24NO_2	449	1.334	**23OMe**	319	1.391
2OMe-5NO_2	347	1.383	**24OMe**	277	1.405
4Me-26NO_2	418	1.332	**25OMe**	295	1.394
2Me-5NO_2	365	1.383	**26OMe**	294	1.398
23Me	321	1.397	**34OMe**	291	1.402
24Me	309	1.399	**35OMe**	327	1.394
25Me	319	1.396	**2OMe-4Et**	293	1.399
26Me	322	1.395	**2OMe-4CHO**	343	1.362
34Me	310	1.399	**246Me**	303	1.400
35Me	326	1.396	**246Cl**	370	1.374
4Me-3NO_2	354	1.386			

by means of the expensive composite *ab initio* G4 method. It is preferable to predict electrochemical values with the use of a known line trend derived from a correlation with experimental values, as opposed to calculating them from a principal equation. As it has been demonstrated in context of mono-substituted derivatives, empirical substituent constants can be employed to a certain extent to determine the relationship with the quantity of interest. In certain cases, the requisite linear trend may not be observed within the available quantities. Moreover, Hammett constants and available experimental values were used to evaluate the trends. Consequently, more sophisticated calculation methods are required. However, it should be noted that the C—N bond length used in the correlation were calculated in the very first step of G4, at simple B3LYP/6-31G(2df,p) level of theory. While the G4 method is expected to yield highly accurate energies, concerns may arise regarding the precision of the solvation model employed. Additional DFT-D3 calculations revealed a similar discrepancy in comparison with experimental data, thereby confirming the limitations of the implicit model. It can be concluded that the knowledge of calculated ΔG value for all studied aniline derivatives in combination with the linear Eq. 6 allows for reasonable determination of electrochemical potential in water.

Acknowledgement
This paper has been supported by the Ministry of Education, Science, Research and Sport of the Slovak

Republic, project VEGA 1/0461/21. We are grateful to the HPC centre at the Slovak University of Technology in Bratislava, which is a part of the Slovak Infrastructure of High-Performance Computing (SIVVP project, ITMS code 26230120002, funded by the European region development funds, ERDF) for the computational time and resources made available.

References

Anjalin M, Kanagathara N, Baby Suganthi AR (2020) Mater. Today Proc. 33: 4751–4755.

Bakalbassis EG, Lithoxoidou AT, Vafiadis AP (2003) J. Phys. Chem. A. 107(41): 8594–8606.

Bannwarth C, Caldeweyher E, Ehlert S, Hansen A, Pracht P, et al. (2021) Wiley Interdiscip. Rev. Comput. Mol. Sci. 11(2): 1–49.

Bannwarth C, Ehlert S, Grimme S (2019) J. Chem. Theory Comput. 15(3): 1652–1671.

Biela M, Kleinová A, Uhliar M, Klein E (2023) J. Mol. Graph. Model. 122: 1–6.

Busch M, Ahlberg E, Ahlberg E, Laasonen K (2022) ACS Omega. 7(20): 17369–17383.

Curtiss LA, Redfern PC, Raghavachari K (2007) J. Chem. Phys. 127(12): 1–8.

Fifen JJ (2013) J. Chem. Theory Comput. 9(7): 3165–3169.

Frisch MJ, Trucks GW, Schlegel HB, Scuseria GE, Robb MA, Cheeseman JR, Scalmani G, Barone V, Mennucci B, Petersson GA, Nakatsuji H, Caricato M, Li X, Hratchian HP, Izmaylov AF, Bloino J, Zheng G, Sonnenberg JL, Hada M, Ehara M, Toyota K, Fukuda R, Hasegawa J, Ishida M, Nakajima T, Honda Y, Kitao O, Nakai H, Vreven T, Montgomery JA Jr., Peralta JE, Ogliaro F, Bearpark M, Heyd JJ, Brothers E, Kudin KN, Staroverov VN, Keith T, Kobayashi R, Normand J, Raghavachari K, Rendell A, Burant JC, Iyengar SS,Tomasi J, Cossi M, Rega N, Millam JM, Klene M, Knox JE, Cross JB, Bakken V, Adamo C, Jaramillo J, Gomperts R, Stratmann RE, Yazyev O, Austin AJ, Cammi R, Pomelli C, Ochterski JW, Martin RL, Morokuma K, Zakrzewski VG, Voth GA, Salvador P, Dannenberg JJ, Dapprich S, Daniels AD, Farkas O, Foresman JB, Ortiz JV, Cioslowski J and Fox DJ (2009) Gaussian 09, Revision D.01, Gaussian, Inc. Wallingford CT.

Fu Y, Liu L, Yu HZ, Wang YM, Guo QX (2005) J. Am. Chem. Soc. 127(19): 7227–7234.

Grimme S, Ehrlich S, Goerigk L (2011) J. Comput. Chem. 32(7): 1456–1465.

Hansch C, Leo A, Taft R (1991) Chem. Rev. 91: 165–195.

Ho J, Coote LM, Cramer CJ, Truhlar DG (2016) In Organic Electrochemistry, pp. 229–259. CRC Press. 5th ed.

Ishikawa A, Nakai H (2016) Chem. Phys. Lett. 650: 159–164.

Jmol development team. (2016) Jmol: an open-source Java viewer for chemical structures in 3D (14.6). http://jmol.sourceforge.net/.

Kleinová A, Biela M, Lukeš V, Klein E (2024) J. Mol. Struct. 1303: 137646.

Kováčová A (2024) Acta Chim. Slovaca. 17(1): 12–21.

Kováčová A, Michalík M, Hartmann H, Lukeš V (2023) J. Mol. Liq. 389: 122811.

Lukeš V, Hartmann H (2021) Color. Technol. 137(4): 389–398.

Lukeš V, Rapta P, Idzik KR, Beckert R, Dunsch L (2011) J. Phys. Chem. B. 115(13): 3344–3353.

Marenich AV, Cramer CJ, Truhlar DG (2009) J. Phys. Chem. B. 113(18): 6378–6396.

Pavitt AS, Bylaska EJ, Tratnyek PG (2017) Environ. Sci. Process. Impacts. 19(3): 339–349.

Pracht P, Bohle F, Grimme S (2020) Phys. Chem. Chem. Phys. 22(14): 7169–7192.

Rani M, Shanker U (2017) J. Environ. Chem. Eng. 5(6): 5298–5311.

Rappoport Z (2007) The chemistry of Anilines, Part 1, Vol. 11 New York: Wiley. 1163.

Skákalová V, Lukeš V, Breza M (1997) Macromol. Chem. Phys. 198(10): 3161–3172.

Takahata Y, Chong DP (2005) Int. J. Quantum Chem. 103(5): 509–515.

Vagánek A, Rimarčík J, Ilčin M, Škorňa P, Lukeš V, Klein E (2013) Comput. Theor. Chem. 1014: 60–67.

Weigend F, Ahlrichs R (2005) Phys. Chem. Chem. Phys. 7(18): 3297–3305.